Korean J. Chem. Eng., 37(9), 1445-1452 (2020)
DOI: 10.1007/s11814-020-0601-7

pISSN: 0256-1115
eISSN: 1975-7220

RAPID COMMUNICATION

Adsorption of dyes from water by *Prunella vulgaris* stem and subsequent fungal decolorization

Xueying Zhang*, Jun Zhou, Yuben Fan***, and Jiayang Liu*,†**

*School of Environmental Science and Engineering, Nanjing Tech University, Nanjing 211816, China
**College of Biotechnology and Pharmaceutical Engineering, Nanjing Tech University, Nanjing 211816, China
***College of Biotechnology, Huanghuai University, Zhumadian 463000, China
(*Received 26 March 2020 • Revised 27 May 2020 • Accepted 3 June 2020*)

Abstract−The residue of herbaceous *Prunella vulgaris* stem (PVS) was evaluated as a potential adsorbent for dye removal, followed by fungal cultivation to achieve dye degradation on solid waste. PVS was analyzed in terms of nutritional composition such as fiber, ash, protein, and fat, which not only played a role in dye adsorption but also provided solid matrix for fungal growth. Five dyes, namely, crystal violet (CV), methylene blue (MB), reactive black 5 (RB), indigo carmine (IC), and direct red 80 (DR), were tested as adsorbates but only CV and MB were effectively adsorbed. Effect of sorbent dose, contact time, dye concentration, and NaCl on adsorption was investigated individually. Langmuir model was suitable for fitting MB adsorption, while adsorption of CV adopted the Freundlich model. The adsorption capacity was calculated to be 625 mg/g for CV and 303 mg/g for MB, respectively. The adsorption process of both dyes was spontaneous and endothermic, and the adsorption followed pseudo 2nd order kinetic model and film diffusion model. The dyed PVS was finally cultivated with fungus *Pycnoporus* sp., wherein efficient dye decolorization was attained under solid state fermentation. As such, PVS coupled with subsequent fungal degradation might serve as novel alternative for dye effluent treatment.

Keywords: Adsorption, *Prunella vulgaris*, Crystal Violet, Methylene Blue, Dye Removal

INTRODUCTION

Prunella vulgaris, a popular medicinal plant and commonly named as "self-heal", has a variety of natural biologically-active compounds with numerous medicinal properties such as antiviral, antioxidant, and antibacterial to treat inflammation and rheumatoid arthritis [1], and even cancer [2]. The highly adaptable plant is widely distributed in many parts of China, especially in central and southeast areas such as Henan and Anhui province. Meanwhile, the edible herb can be seen in other countries [3]. During spica (seed and flower) harvesting for medical purposes, *Prunella vulgaris* stem (denoted as PVS herein) is thereupon left and discarded as useless waste and presents a disposal concern. PVS could be 20-30 cm in length and accounts for 50% of the total plant dry mass as shown in Fig. 1. PVS in itself is supposed to be similar to numerous lignocellulosic wastes that have already been extensively employed as adsorbents [4,5], but its ability in adsorbing dye molecules has not been reported yet. This study was conceived and conducted on the basis of the possibility that PVS is a potential dye adsorbent like other agro-wastes and, most importantly, on the fact that a number of small-scale dyeing mills are located in or nearby its planting areas in some provinces of China. Our field investigations show that the dye effluent without any treatment is still discharged into nearby lands or creeks, inevitably posing great threat to the surrounding eco-system [6]. Apart from the lack of or limited supervision by local authorities, high treatment cost in facilities and operation would be a giant hindrance for such mills with very low profit [7]. It is, therefore, of great significance for those mills to acquire some cheap and easily operated treatment schemes, among which adsorption technology obviously emerges as an effective alternative [7,8]. As such, the cheapest adsorbent materials will go to agro-wastes at hand to be readily collected and with little processing. Researchers have recently fabricated novel catalytic composites or polymers (e.g., Fe_3O_4/AC/CD/Alg offering 99.5% removal of methylene blue in just 90 min) [9-11], and may also have been familiar with valorization of some agro-wastes, e.g., *Azolla pinnata* [12], wheat straw [13], and soybean and rice hulls [14] for dye removal, laying a good theoretical foundation for such technique. In addition to raw lignocellulosic materials, they could be used in modified form to render enhanced performance [15]. However, far fewer are aware of PVS regarding its potential and mechanism involved in removing dyes from water. Moreover, the dye adsorbed PVS can be a new challenge if not properly treated. This study deals with characterization of PVS and dye removal efficiency under various conditions in association with several adsorption models building and analysis. Further, biological decolorization of fixed dyes on PVS was evaluated with solid state fermentation.

MATERIALS AND METHODS

1. Chemicals, Sorbent Material and Fungal Culture

Five dyes of analytical grade, i.e., two cationic dyes crystal violet (CV) and methylene blue (MB), three anionic dyes reactive black 5 (RB), indigo carmine (IC), and direct red 80 (DR), were purchased

†To whom correspondence should be addressed.
E-mail: jyliu@njtech.edu.cn

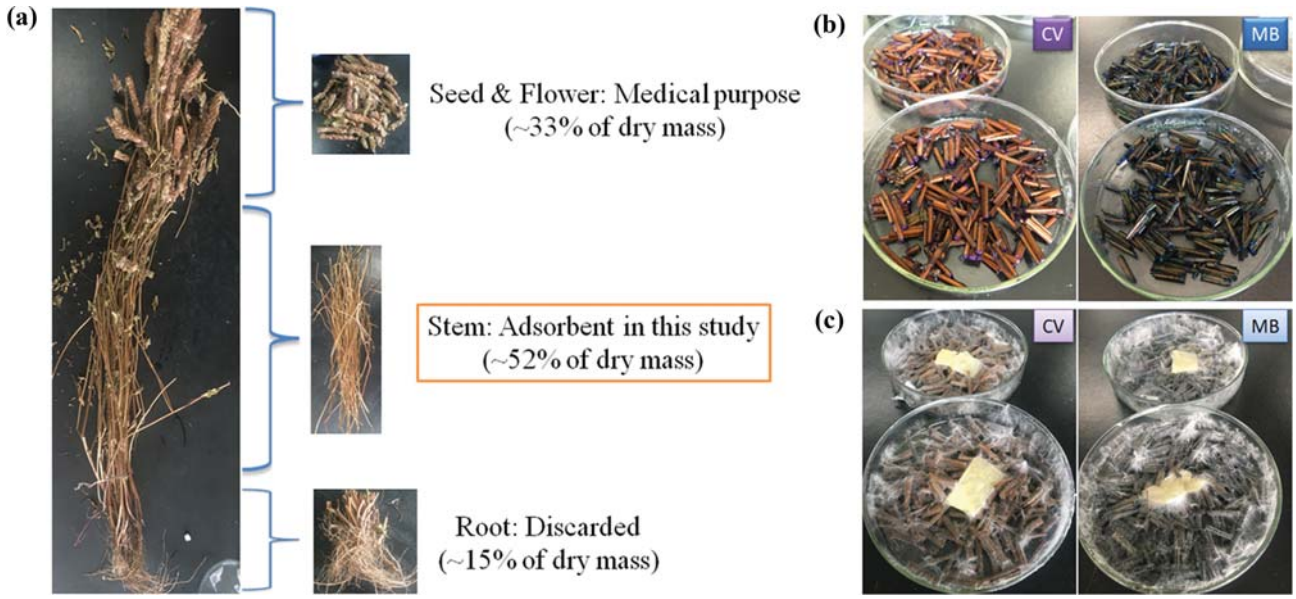

Fig. 1. Whole plant and usage of each part (a), PVS loaded with dye before (b) and after fungal cultivation of 14 days (c).

Table 1. Basic information of five dyes used in this study

Dye	Formula	Structure	MW (g/mol)	λ_{max} (nm)
CV	$C_{25}H_{30}N_3Cl$	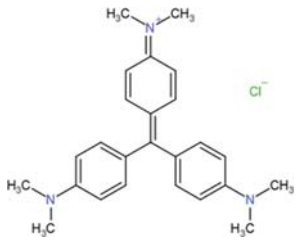	407.98	584
MB	$C_{16}H_{18}ClN_3S$	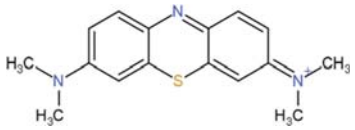	319.85	665
RB	$C_{26}H_{21}N_5Na_4O_{19}S_6$	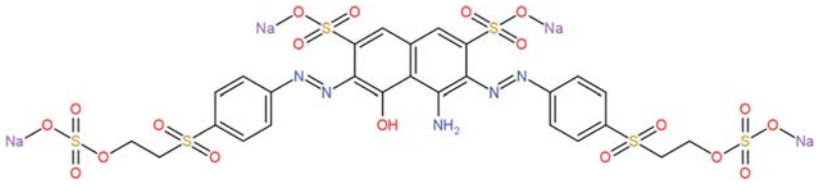	991.82	597
IC	$C_{16}H_8N_2Na_2O_8S_2$	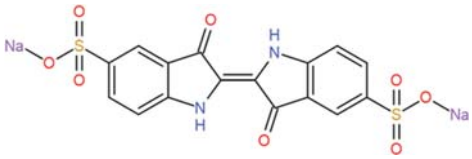	466.35	610
DR	$C_{45}H_{26}N_{10}Na_6O$	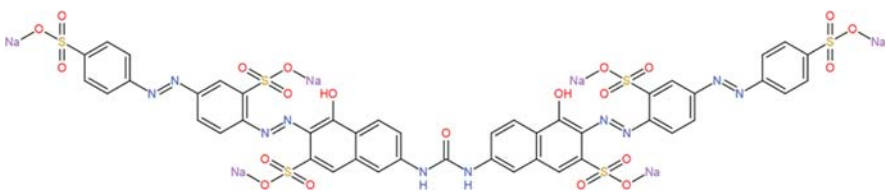	1373.07	530

from Sigma-Aldrich (St. Louis, Mo, USA). Each dye was dissolved in deionized water to a concentration of 50 mg/L for adsorption study except that for varied initial dye concentration effect study. The pH values of these dye solution for further adsorption remained natural as they were unless otherwise stated. The maximum absorbance wavelength of CV and MB solution was 584 nm and 665 nm [16], respectively, while the other three dye solutions were subjected to full wavelength scanning with a spectrophotometer to obtain individual maximum absorption: λ_{max}(RB)=597 nm, λ_{max}(IC)=610 nm, and λ_{max}(DR)=530 nm (Table 1). Based on the linear relationship between absorption and corresponding dye concentration, standard curves were made to determine the residual amount of dye after adsorption in the following experiments. Other chemicals used herein were purchased from Sinopharm Chemical Reagent Co., Ltd (Shanghai, China).

Dry whole plants were collected from a local planting area in Zhumadian of central China, and the stem (PVS) was manually cut off with a scissor and washed with tap water to remove the dirt and soluble matters (Fig. 1(a)), followed by a natural air-drying process for a couple of days. The clean dried PVS was then ground into powder with a bench grinder and passed through a screen of 0.5 mm for further use. *Pycnoporus* sp., used in this study to decolorize the sorbed dyes on PVS, was a stock fungal culture with great potential for submerged and solid state fermentation in some of our previous publications [16,17]. The fungus was subcultured on new potato dextrose agar (PDA) every month to remain active for immediate use.

2. Characterization of PVS

To better know the herb waste, the air-dried PVS was subjected to nutritional composition analysis, including crude fiber, crude protein, crude fat, and crude ash [18]. Fourier transform infrared (FTIR) spectra were obtained by scanning PVS (prepared as potassium bromide pellet) with Nicolet iS10 FT-IR spectrometer (Thermo Fisher, USA) in the range of 4,000-400 cm^{-1}.

3. Adsorption Study

Dye adsorption was basically carried out in 250 mL flask containing 50 mL dye solution at condition of: dye concentration (50 mg/L), sorbent dosage (2 g/L), contact time (4 h), rotation shaking speed 100 rpm, and temperature (25 °C). The effect of these variables on dye removal rate was established using one-at-a-time strategy by adjusting dimension of only one parameter while keeping other variables unchanged. Effect of NaCl ranging from 0-1 mol/L was also examined in the basic adsorption condition. pH values of dye solutions were adjusted to be within 3 to 9 using diluted HCl and NaOH solution. After adsorption, the solution in each flask was centrifuged at 4,000 rpm for 10 min to obtain the supernatant in which residual dye concentration was determined. Dye removal rate (1) and amount of dye adsorbed on PVS at equilibrium (q_t) (2) were calculated as follows:

$$R = \frac{c_0 - c_t}{c_0} \times 100\% \quad (1)$$

$$q_t = \frac{(c_0 - c_t) \times V}{W} \quad (2)$$

where c_0 is initial dye concentration (mg/L); c_t is dye concentration (mg/L) at time t; V is volume of dye solution (L); W is weight of adsorbent (g); q_t is adsorption amount (mg/g) at time t. All sorption experiments were performed in triplicate with relative standard deviation <5% and the averages for triplicate data were reported in the results.

4. Kinetic Model

The data obtained from time effect profile were fitted with Lagergren's pseudo-first-order model (3) and Ho's pseudo-second-order model (4)

$$\lg(q_e - q_t) = -\frac{K_1 t}{2.303} + \lg q_e \quad (3)$$

$$\frac{t}{q_t} = \frac{t}{q_e} + \frac{1}{K_2 q_e^2} \quad (4)$$

where q_e is equilibrium dye adsorption amount (mg/g); q_t is adsorption amount (mg/g) at contact time t (h or min); K_1 is the equilibrium rate constant of the first order sorption (min^{-1}); K_2 is the equilibrium rate constant of the second order sorption (g/mg·min).

To study the sorption mechanism, the adsorption data were also fitted with film diffusion model (5) and intraparticle diffusion model (6):

$$\ln\left(1 - \frac{q_t}{q_e}\right) = -K_3 t \quad (5)$$

$$q_t = K_4 t^{1/2} + C \quad (6)$$

where q_e is equilibrium dye adsorption amount (mg/g); q_t is adsorption amount (mg/g) at contact time t (h or min); K_3 is equilibrium rate constant (min^{-1}); K_4 is intraparticle rate constant (mg/g·$min^{1/2}$); C is film diffusion extent (mg/g).

5. Isotherm Model

The Langmuir (7) and Freundlich (8) equations were employed to explicate the sorption isotherms using the data obtained from dye concentration effect profile.

$$\frac{C_e}{q_e} = \frac{1}{K_a q_m} + \frac{C_e}{q_m} \quad (7)$$

$$\lg q_e = \frac{1}{n}\lg C_e + \lg K_F \quad (8)$$

where K_a (L/mg) is the Langmuir adsorption constant and q_m (mg/g) is the maximum dye amount of adsorption corresponding to complete monolayer coverage on the surface, q_e (mg/g) is the amount of dye adsorbed by sorbent at equilibrium, and C_e (mg/L) is the equilibrium concentration of dye solution. K_F is an indicator of adsorption capacity (mg/g) and 1/n is the adsorption intensity.

6. Thermodynamic Model

The change in free energy (ΔG^o) was evaluated using the data obtained from temperature effect profile and the following equation to study the thermodynamic nature:

$$\Delta G^o = -RT\ln\left(\frac{q_e}{c_e}\right) \quad (9)$$

where R is gas constant (8.3143 J·mol^{-1}·K^{-1}); T is absolute temperature (Kelvin); q_e is equilibrium adsorption amount (mg/g); c_e is equilibrium dye concentration (mg/L). From the plot of ΔG^o vs. T, the value of enthalpy ΔH^o and entropy ΔS^o can be calculated as

follows.

$$\Delta G^o = \Delta H^o - T\Delta S^o \quad (10)$$

7. Fungal Degradation

To promote fungal colonization under better aeration, PVS was cut into short sticks with length of 0.5-1 cm for dye adsorption rather than ground into powder. Two grams of PVS sticks loaded with dye CV (Qe=1.39 mg/g) or MB (Qe=2.36 mg/g) after dye adsorption was placed onto glass petri dish with moisture of ~70% and then was autoclaved at 121 °C for 20 min (Fig. 1(b)). Pure fungal culture of actively growing *Pycnoporus* sp. on PDA plate was cut into squares (or wedges of 1 cm×1 cm) from the velvet margin of the colony and 1 square was inoculated in the center of such sterilized but cooled PVS and then cultivated at static condition at 30 °C for two weeks [19]. Upon the completion of cultivation (Fig. 1(c)), the residue was extracted with ethanol to quantify the remaining dye with spectrophotometry as above described [20]. Dye loaded PVS without fungal cultivation served as control. Decolorization rate was the removed dye amount out of that in control sample. Three replicates of cultivation were conducted.

RESULTS AND DISCUSSION

1. Characterization of PVS

Before the adsorption study, adsorbent PVS was first characterized with regard to its nutritional composition as well as its FTIR spectra with or without loading of dyes. As demonstrated in Fig. 2(a), air-dried PVS is roughly comprised of 60.4% fiber, followed by 13.4% ash, 7.6% protein, and 1.6% fat. Certain amount of moisture, i.e., 17%, was still present in the material since it was not oven-dried at 100 °C overnight. The composition of PVS slightly differs from those of peanut shell and oiltea shell, but still potentially is a source for fungal natural medium [16,21]. The PVSs with or without loading of dye were then analyzed with FTIR spectra as shown in Fig. 2(b). Some typical absorbance peaks of PVS corresponding to the complex functional sites on the surface were observed, in particular at wavelength around 3,400, 2,900, 1,040-1,750, and 500 cm^{-1}. Absorbance peak at 3,400 cm^{-1} denotes the presence of -OH derived from cellulose in PVS, while absorbance at 2,900 cm^{-1} is the result of vibration of C-H [22]. C=O stretching of -COOH in ester, carbonyl and/or carboxyl group in cellulose may generate a narrow peak around 1,700 cm^{-1} [23]. Stretching vibration of C-O-C in cellulose and hemicellulose is reflected at around 1,000 cm^{-1} [24]. The region of <1,000 cm^{-1} explains the presence of heterocyclic aromatics in lignin. The adsorption intensity at all these peaks showed significant changes, a strong indication of successful adsorption of CV and MB onto PVS.

2. Effect of Influencing Parameters on Dye Adsorption by PVS

Dye removal efficiency by PVS under a series of varying conditions is depicted in Fig. 3. Among five dyes in Fig. 3(a), only cationic dye CV and MB were effectively removed from water without adjusting pH value over 24-h reaction, reaching approximately 85% and 95%, respectively. Failure of adsorption of dye RB, DR, and IDA was presumably because of their nature of anionic dye and having larger molecular weights than CV and MB, as described in Table 1. The -COOH on the surface of PVS may help account for the adsorption of CV and MB (Fig. 2(b)). Some agro-wastes like peanut shell have been reported to have negative zeta potential, making them effective in attracting cationic dyes [16]. When the solution pH values were adjusted to acidic range, weak adsorption of RB, DR, and IDA occurred, e.g., reaching around 35% removal at pH 3 (data now shown here), likely due to electrostatic interaction [5]. Fast adsorption of the two dyes on PVS took place at the beginning of the process and the equilibrium was reached within 4 h. Particularly, 75% CV and 91% MB were removed in just 10 min, respectively (Fig. 3(a)). Increasing initial dye concentration had different effect on dye removal, specifically, CV removal was on the increase while MB removal on the decrease (Fig. 3(b)). It is interesting that as high as 90% removal was attained for MB and CV by PVS even at high initial dye concentration of 400 mg/L, much better that raw eucalyptus barks whose percentage removal decreased to 38% when MB concentration increased up to 70 mg/L [5]. Temperature increasing from 10 to 60 °C seemed to have a weak stimulating effect on CV removal, but almost none on MB removal (Fig. 3(c)), suggesting environmental temperature is not a big consideration in practical application. As can be seen from Fig. 3(d), adsorbent amount did play a role in dye removal, especially being dosed below 1 g/L. Clearly, more PVS to be applied would result into more dye to be removed. In a range of concentration 0-1 mol/L, NaCl had quite different effect on dye removal, i.e., CV

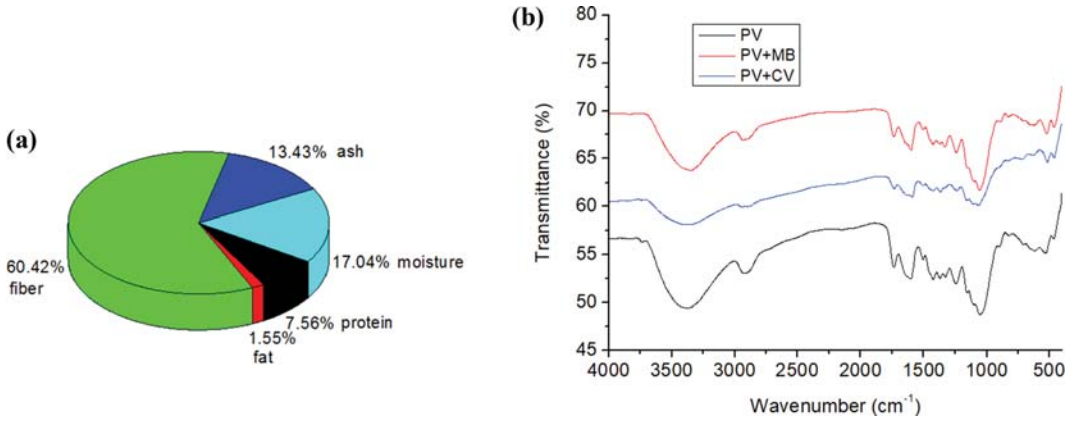

Fig. 2. Nutritional composition of PVS and FTIR spectra of PVS with or without loading of dyes.

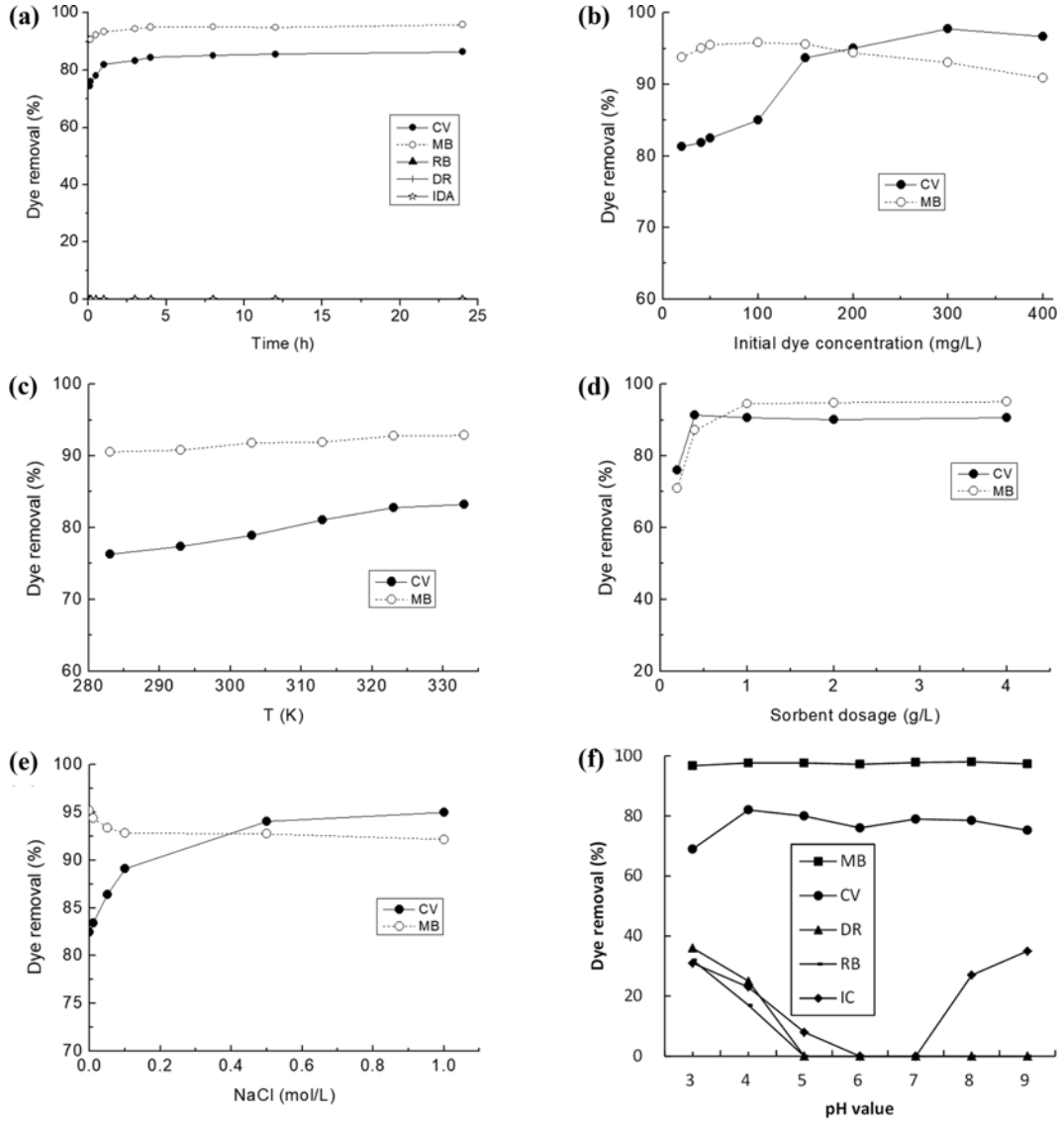

Fig. 3. Effect of influencing parameters on dye adsorption by PVS.

removal increased from 82% to 95% while MB removal decreased from 95% to 92% (Fig. 3(e)). Sodium has been reported in the range of hundred to thousand mg/L as the most abundant metal in textile wastewater, which could be hundred times higher than the other ones [25]. The result herein shows very little effect of tested sodium concentrations on dye removal by PVS, which is a good sign for real application. Removal of CV may also follow a decreasing trend as salt concentration increases by some adsorbents, such as modified phoenix tree [5]. The effect of pH value on dye removal was also examined, in particular with the intention to check if PVS had potential of adsorbing three other dyes if acidity of solution changed. Fig. 3(f) shows that only acidic condition seems to offer removal of DR, RB, and IC but still in relatively low efficiency (i.e., no greater than 40% at pH 3), while both MB and CV performed very well in all the pH ranges tested. No significant variation in pH value among solutions was observed after dye adsorption by PVS. 90-98% removal of MB was reported within pH range 4-10 using sugarcane bagasse as adsorbent [26]. Generally, the manner in which CV and MB adsorption was affected by these factors is in good accordance with some reports, such as using peanut shell [16]. Since PVS was studied for the first time, its capability of removing dyes from water, as demonstrated above, thus further expands the source of lignocellulose-based bio-adsorbent.

3. Adsorption Isotherms

Based on the data in Fig. 2(b), two isotherm models of Langmuir and Freundlich, were built in Fig. 4 and the related model parameters were calculated and listed in Table 2. The two models describe adsorption occurring on homogeneous and heterogeneous surfaces, respectively [27]. From correlation coefficient, CV and MB sorption by PVS followed Freundlich and Langmuir model, respectively, implying adsorption of the two dye might adopt different manners. Dye MB fell behind CV in terms of their adsorption capacity calculated from Langmuir model (q_m=625 mg/g for CV, q_m= 303 mg/g for MB), as presented in Table 2. In this regard, PVS is obviously better than most of the reported lignocellulosic materials towards CV, such as sugarcane bagasse (30.7 mg/g) [26], pea-

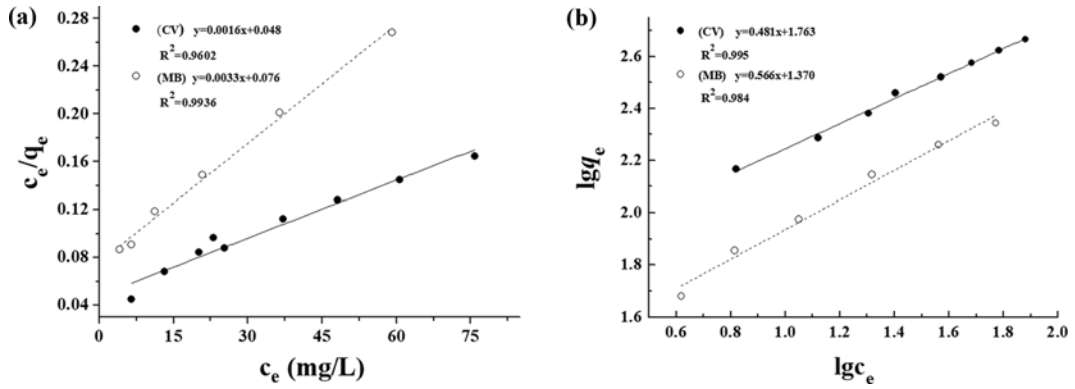

Fig. 4. Langmuir model (a) and Freundlich model (b) for CV and MB by PVS.

Table 2. Parameters of Langmuir and Freundlich isotherms for CV and MB by PVS

Langmuir isotherm			Freundlich isotherm		
Parameter	CV	MB	Parameter	CV	MB
q_m (mg/g)	625	303	n^{-1}	0.481	0.566
K_L (L/mg)	0.033	0.043	K_F (mg/g)	57.94	23.44
R^2	0.9602	0.9936	R^2	0.995	0.984

nut shell (256 mg/g) [16], and palm kernel fiber (78.9 mg/g) [24], and chemically synthesized materials such as Semi-IPN hydrogels (20-28.6 mg/g) [28], and even comparable to commercial activated carbon (271 mg/g) [23]. Metal-organic framework Uio-66 has been synthesized and used to adsorb MB from water, but only achieved 91 mg/g for its maximum adsorption capacity [29]. Maximum adsorption of around 178 and 84 mg/g has been obtained for CV by natural zeolite and Merck activated carbon, respectively [30], which is apparently lower than that in this study.

4. Adsorption Kinetics and Diffusion Model

Two kinetic models were applied to fit the adsorption process (Fig. 5), and the related parameters are listed in Table 3. It seems that Ho's pseudo-second-order model ($R^2 \approx 1$) can better describe the sorption process, suggesting chemical sorption of CV and MB on PVS [24]. This behavior agrees well with some other adsorbents such as nanocomposite $ZrSiO_4$ NPs -SDS [31] and natural com-

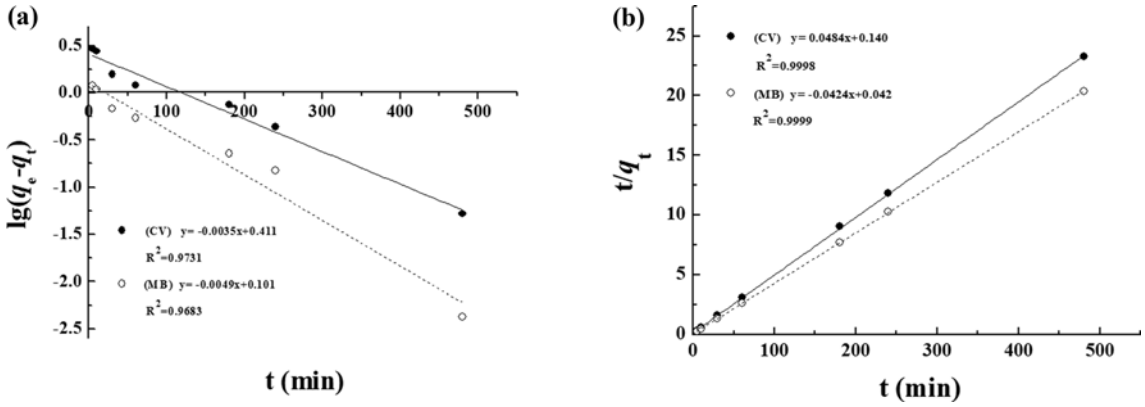

Fig. 5. Lagergren pseudo-first-order (a) and Ho's pseudo-second-order kinetic models (b) for the adsorption of CV and MB by PVS.

Table 3. Parameters for Lagergren pseudo-first-order and Ho's pseudo-second-order kinetic model for the adsorption of CV and MB by PVS

CV		MB	
Pseudo-first-order	Pseudo-second-order	Pseudo-first-order	Pseudo-second-order
R^2=0.9731	R^2=0.9998	R^2=.9683	R^2=0.9999
q_e=2.576	q_e=20.66	q_e=1.2618	q_e=23.58
k_1=0.0081	k_2=0.0484	k_1=0.0113	k_2=0.0424

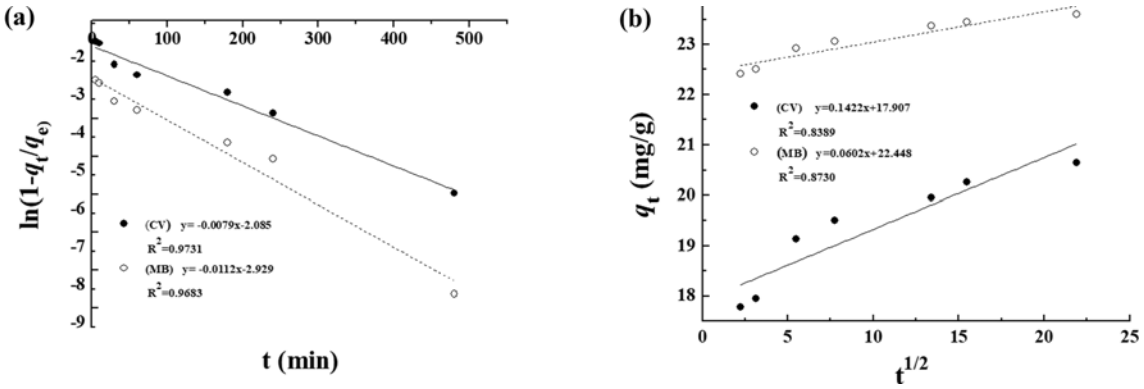

Fig. 6. Film diffusion model (a) and intra-particular diffusion model (b) for the adsorption of CV and MB by PVS.

Table 4. Thermodynamic parameters for CV and MB adsorption by PVS

Dye	ΔS^o KJ/mol·K	ΔH^o kJ/(mol)	ΔG^o (KJ/mol)					
			283 K	293 K	303 K	313 K	323 K	333 K
CV	0.030	7.51	−1.12	−1.31	−1.57	−1.98	−2.36	−2.52
MB	0.031	5.20	−3.70	−3.89	−4.35	−4.53	−5.00	−5.19

posite IMW [32] in adsorbing CV and MB. Besides, the adsorption amount calculated ($q_{e\,cal}$) (Table 3) from Ho's model came closer to those obtained from the experiment ones. It has been reported that most adsorption processes of dyes by agricultural solid materials in either natural or modified forms would take pseudo-first-order model kinetic [5]. Two diffusion models were also applied to fit the adsorption process (Fig. 6). Relatively, film diffusion model was superior to intra-particle diffusion model because the former yielded a higher R^2 value of around 0.97 than the latter for both dyes. Basically, a very rapid dye adsorption to the external surface occurred prior to a slow intra-particle diffusion in the interior of PVS [16].

5. Adsorption Thermodynamics

Table 4 summarizes free Gibbs energy change (ΔG^o) calculated based on Eq. (9) and enthalpy change ΔH^o and entropy change ΔS^o obtained according to Eq. (10) as well as plotting between ΔG^o vs. temperature in Fig. 7 (R^2=0.98). The negative values of ΔG^o for adsorption of both CV and MB onto PVS reveal the favorability of the reaction [33]. Values of ΔG^o for MB seemed a bit smaller than those for CV at the same temperature. The negative values of ΔG^o in combination of positive values of ΔH^o could be a strong indication that the sorption of CV and MB by PVS was spontaneous and endothermic. Adsorptive reaction of CV and MB has also been reported to be endothermic with other agro-adsorbents, such as peanut shell [16] and Eucalyptus *sheathiana* bark [5]. The randomness at the solid-solution interface tends to increase based on the positive values of ΔS^o around 0.03 $KJ \cdot mol^{-1} \cdot K^{-1}$ for the two dyes [34]. The thermodynamic data for CV and MB adsorption by PVs in this study were similar to those obtained for those by coniferous pinus bark powder (CPBP) [35].

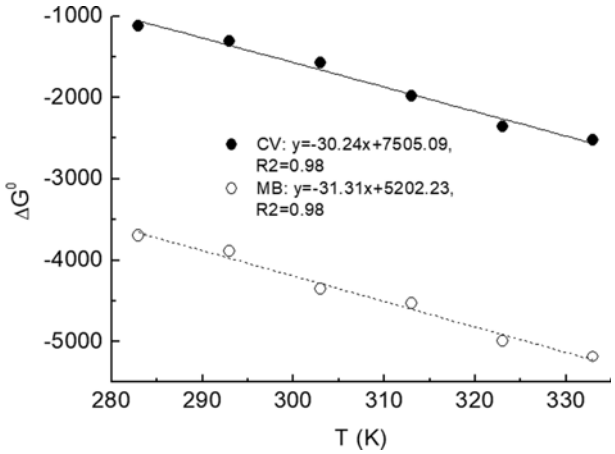

Fig. 7. Plot of ΔG^o (J/mol) vs. temperature (Kelvin) for CV and MB adsorption by PVS.

6. Fungal Degradation of Dye on PVS

Considering adsorbed dyes on PVS might serve as extra carbon source and be depleted, the PVS loaded with dye CV or MB was further cultivated with fungus *Pycnoporus* for two weeks and decolorization was found to be very effective because the color on PVS was visually faded by the fungus (Fig. 1(c)). Specifically, around 91% of CV and 85% of MB (SD<10%) was removed in color by the fungus, respectively (Figure not plotted due to the few sets of data). It seems harder for the fungus to decolorize MB than CV on PVS, possibly caused by their differentiated chemical structures. The nutritional constituents in PVS, as shown in Fig. 1, would allow fungal colonization and promote secretion of lignin-degrading enzymes which might account for the dye degradation. Actually, this fungus has previously exhibited strong transformation ability toward hormones in poultry litter [19]. Similar results have been reported in a recent publication, in which a binary dye (brilliant blue FCF and allura red AC) adsorbed onto corncob was degraded by 80-86% with different white-rot fungi through solid state fer-

mentation due to the activity of a couple of extracellulous ligninolytic enzymes, namely, laccase and manganese peroxidase [36]. Altogether, these experimental results demonstrate the feasibility of fungal removal of organic pollutants on solid matrix or medium, potentially finding its way in practical application in wastewater treatment. Apparently, decolorization or degradation efficiency could vary greatly with changing parameters, e.g., fungal species, nutrient content in solid matrix, enzymatic activities, and types of organics, such experiments should be followed up in future work.

CONCLUSIONS

Untreated agro-wastes are not applicable to all types of dyes, regarding their adsorption from aqueous solution, especially for those anionic dyes. Among five different dyes in the current study, PVS only worked well on cationic dye CV and MB with maximum adsorptive potential of 625 and 303 mg/g for each. Three other anionic dyes were hardly removed by adsorptive process. It is possible in reality that some types of dye effluent adjacent to PVS rich area can be efficiently treated and decolorized with the aid of this cheap adsorbent. Although certain environmental factors may affect dye removal efficiency to some degree, it is recommended that batch adsorption can be performed and finished within 1 h by employing 1 g/L PVS, as the dye concentration in real effluent is, in most cases, not as high as those tested in this study. Solid state cultivation is effective regarding degradation of organic loaded PVS complex and deserves to be tested broadly in future studies.

ACKNOWLEDGEMENTS

This work was financially supported by the National Natural Science Foundation of China (21777069), the National Key Research and Development Program of China (2016YFE0112800), the National Key Research and Development Program of the Ningxia Hui Autonomous Region (2019BFH02008), and the Jiangsu Synergetic Innovation Center for Advanced Bio-Manufacture.

COMPETING INTERESTS

The authors declare that they have no competing interests.

REFERENCES

1. M. Zaka, S. A. Sehgal, S. Shafique and B. H. Abbasi, *J. Mol. Graph. Mod.*, **74**, 296 (2017).
2. H. Y. Lou, L. Jin, T. Huang, D. P. Wang, G. Y. Liang and W. D. Pan, *Tetrahedron Lett.*, **58**, 401 (2017).
3. H. Fazal, B. H. Abbasi, N. Ahmad, M. Ali, S. S Ali, A. Khan and D. Q. Wei, *Artif. Cells Nanomed. Biotechnol.*, **47**, 2553 (2019).
4. Y. Zhou, L. Zhang and Z. Cheng, *J. Mol. Liq.*, **212**, 739 (2015).
5. S. Afroze and T. K. Sen, *Water Air. Soil Poll.*, **229**, 225 (2018).
6. G. Crini, *Bioresour. Technol.*, **97**, 1061 (2006).
7. W. Li, B. Mu and Y. Yang, *Bioresour. Technol.*, **277**, 157 (2019).
8. J. Mo, Q. Yang, N. Zhang, W. Zhang, Y. Zheng and Z. Zhang, *J. Environ. Manage.*, **227**, 395 (2018).
9. X. Xu, A. Geng, C. Yang, S. A. C. Carabineiro, K. Lv, J. Zhu and Z. Zhao, *Ceram. Int.*, **46**, 10740 (2020).
10. S. Yadav, A. Asthana, R. Chakraborty, B. Jain, A. Singh, S. Carabineiro and M. Susan, *Nanomaterials*, **10**, 170 (2020).
11. C. Rodrigues, R. Silva, S. Carabineiro, F. J. Maldonado-Hódar and L. Madeira, *Catalysts*, **9**, 478 (2019).
12. M. R. R. Kooh, L. B. L. Lim, M. K. Dahri, L. H. Lim and J. M. R. Sarath Bandara, *Waste Biomass Valori.*, **6**, 547 (2015).
13. N. S. Trivedi, R. A. Kharkar and S. A. Mandavgane, *Waste Biomass Valori.*, **10**, 1323 (2019).
14. A. M. Rizzuti and D. J. Lancaster, *Waste Biomass Valori.*, **4**, 647 (2013).
15. M. Perez-Ameneiro, G. Bustos, X. Vecino, L. Barbosa-Pereira, J. M. Cruz and A. B. Moldes, *Water Air. Soil Poll.*, **226**, 133 (2015).
16. J. Liu, Z. Wang, H. Li, C. Hu, P. Raymer and Q. Huang, *Bioresour. Technol.*, **249**, 307 (2018).
17. J. Liu, Z. Yu, X. Liao, J. Liu, F. Mao and Q. Huang, *J. Clean. Prod.*, **127**, 600 (2016).
18. G. Koutrotsios, K. C. Mountzouris, I. Chatzipavlidis and G. I. Zervakis, *Food Chem.*, **161**, 127 (2014).
19. J. Liu, Q. Luo and Q. Huang, *J. Clean. Prod.*, **139**, 1400 (2016).
20. J. X. Yu, R. A. Chi, X. Z. Su, Z. Y. He, Y. F. Qi and Y. F. Zhang, *J. Hazard. Mater.*, **177**, 222 (2010).
21. J. Liu, E. Li, X. You, C. Hu and Q. Huang, *Sci. Rep.*, **6**, 38450 (2016).
22. S. Afroze, T. K. Sen, M. Ang and H. Nishioka, *Desalin. Water Treat.*, **57**, 5858 (2016).
23. D. D. Sewu, P. Boakye and S. H. Woo, *Bioresour. Technol.*, **224**, 206 (2017).
24. G. O. El-Sayed, *Desalination*, **272**, 225 (2011).
25. D. A. Yaseen and M. Scholz, *Int. J. Environ. Sci. Te.*, **16**, 1193 (2019).
26. Z. Zhang, I. M. O'Hara, G. A. Kent and W. O. S. Doherty, *Ind. Crop. Prod.*, **42**, 41 (2013).
27. X. Xu, B. Bai, H. Wang and Y. Suo, *J. Phys. Chem. Sol.*, **87**, 23 (2015).
28. S. Li, *Bioresour. Technol.*, **101**, 2197 (2010).
29. A. A. Mohammadi, A. Alinejad, B. Kamarehie, S. Javan, A. Ghaderpoury, M. Ahmadpour and M. Ghaderpoori, *Int. J. Environ. Sci. Te.*, **14**, 1959 (2017).
30. M. Sarabadan, H. Bashiri and S. M. Mousavi, *Korean J. Chem. Eng.*, **36**, 1575 (2019).
31. M. E. Mahmoud, G. M. Nabil, M. A. Khalifa, N. M. El-Mallah and H. M. Hassouba, *J. Environ. Chem. Eng.*, **7**, 103009 (2019).
32. J. Liu, F. Chen, C. Li, L. Lu, C. Hu, Y. Wei, P. Raymer and Q. Huang, *J. Clean. Prod.*, **208**, 552 (2019).
33. M. T. Yagub, T. K. Sen, S. Afroze and H. M. Ang, *Adv. Colloid Interface Sci.*, **209**, 172 (2014).
34. L. B. L. Lim, N. Priyantha, H. I. Chieng and M. K. Dahri, *Desalin. Water Treat.*, **57**, 5673 (2016).
35. R. Ahmad, *J. Hazard. Mater.*, **171**, 767 (2009).
36. A. Merino-Restrepo, F. Mejía-Otálvaro, C. Velásquez-Quintero and A. Hormaza-Anaguano, *J. Environ. Manage.*, **254**, 109805 (2020).